

behavior (Figure 3.11).

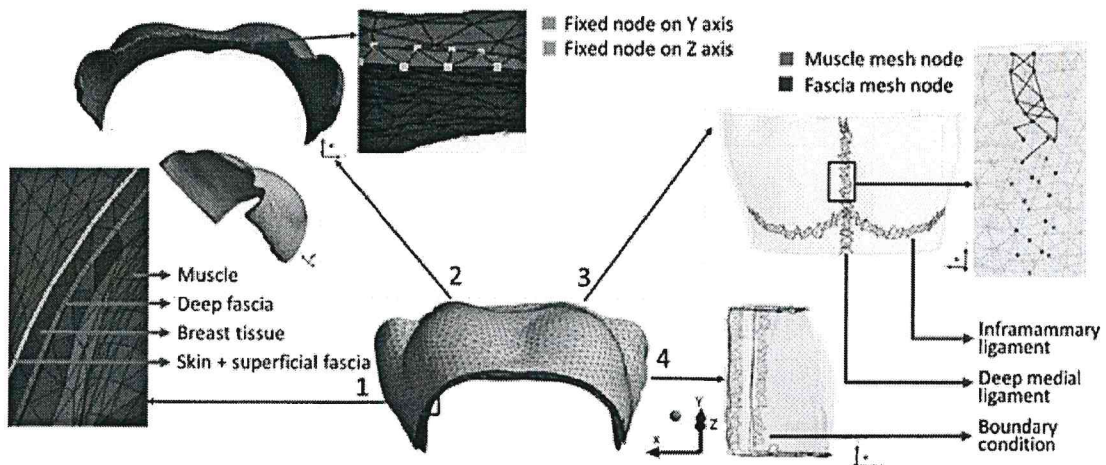


Figure 3.11: Components of the finite elements mesh.

The deep layer of superficial fascia is much stiffer than underlying adipose tissues. Due to imposed boundary conditions, the amount of sliding depends on the fascia's elasticity. The suspensory ligaments define regions where the breast sliding is minimal regardless of applied deformations. These additional stiff structures reduce the tissues sliding and improve the solution convergence capability.

### 3.6 Materials constitutive models

The final model consists of 6 types of tissues, wherein 4 tissues (glandular, fatty, muscle and skin) are well described and regularly used for biomechanical modeling and 2 of them (fascia and suspension ligaments) with limited use and poorly described in literature. A large range of constitutive parameters are available for each tissue, however because of an inconsistent interindividual variability, patient-specific parameters have to be identified.

Here, all materials except the suspensory ligaments are modeled using the Neo-Hookean potential function. Breast ligaments are considered as linear materials. Subject-specific mechanical tissue properties are computed using an optimization process based on a multi-gravity loading simulation procedure (Figure 3.12). First, for a given set of parameters ( $\lambda_{breast}, \lambda_{muscle}, \lambda_{skin}, \lambda_{fascia}, \lambda_{ligam}, \nu$ ) the breast stress-free configuration is estimated by minimizing the difference between the simulated and measured breast geometry in prone configuration. Then, from the new estimated stress-free geometry, the supine breast configuration is derived. The estimated supine geometry is compared to the measured one using modified Hausdorff distance, thus representing the estimation error. To avoid taking into account the geometry dissimilarity due to arms position, the modified Hausdorff distance is computed only on breast skin surface. The process implies multiple simulation based on imposed nodes displacement; therefore the FE mesh can be significantly altered before

reaching an optimal stress-free geometry. Mainly for that reason we chose to perform an exhaustive manual rather than an automatic research of the optimal set of constitutive parameters.

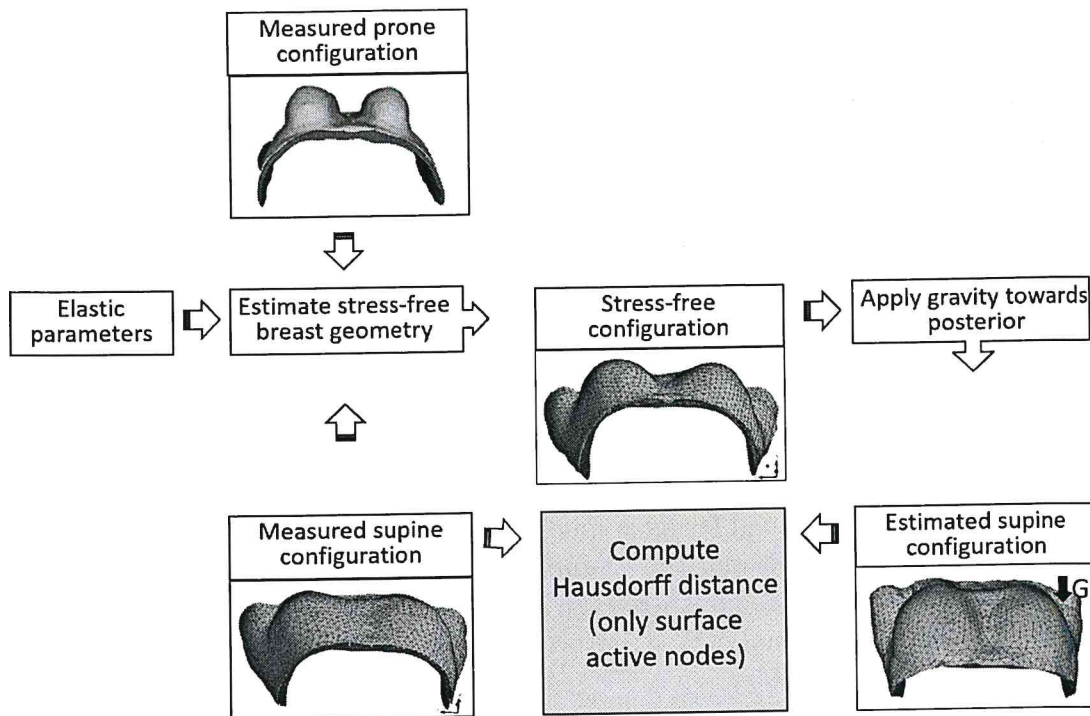


Figure 3.12: Process to estimate optimal material parameters

An optimization process including finite elements simulation with 6 parameters results  
1620 is a complex and time-consuming problem. The model simplification is then performed in two steps. First, the parameters which variations have non-significant effects on simulation results are identified and set to an optimal fixed value. Next for parameters which variations have a high impact, a sensitivity study is performed to redefine the search intervals and interval's discretization step.

### 1625 3.6.1 Model simplification

The breast tissues are mainly composed of water; an usual assumption is to consider them as nearly incompressible materials (Fung, 2013). However, previous works proposed a Poisson's ratio value ranging between  $\nu = 0.3$  (Hopp et al., 2013) and  $\nu = 0.5$  (Gamage et al., 2012). In a multi-loading gravity simulation, the breast volume is nearly constant, thus, the influence of Poisson's ratio on nodes displacements is studied only for values laying between  $\nu = [0.45, 0.495]$  (Figure 3.13).

The simulations were performed by applying the gravity force in postero-anterior direction on breast geometry from supine configuration. On the right-hand side, the mean and the maximal displacement of the skin nodes is given for each values of  $\nu$ . On the left-hand side

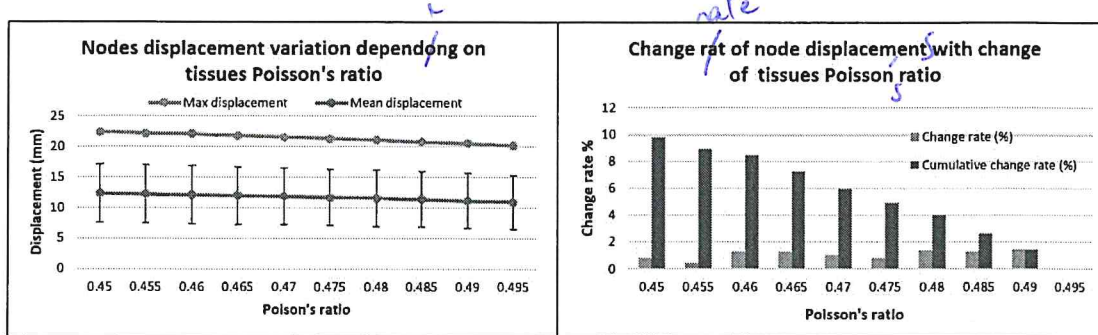


Figure 3.13: Process to estimate optimal material parameters

side the maximal difference of nodal displacement between two consecutive simulations (change rate) and and the maximal difference of node displacement between the actual and the less deformed geometry (cumulative change rate) are plotted. The change rate is computed within the assumption that the maximal displacement over the simulations set represents 100% change rate. Non-significant variations are observed on the mean and maximal displacements of skin nodes, thus a constant value of  $\nu = 0.49$  was chosen.

The pectoral muscle together with the thoracic cage are the breast tissues support, under gravity loading the muscle deformation is neglected. Therefore, its Young's modulus was not included on the parametric study and was chosen large enough so that only minimal deformations occur ( $\lambda_{muscle} = 10kPa$ ). (je veux pas si grande puissance)

The ligamentous breast structures are added with a cable-like behavior to reduce tissues sliding. Their Young's modulus is also not included in the optimization process and is set sufficiently high ( $\lambda_{ligam} = 500kPa$ ) to preclude their elastic deformation.

The adipose and glandular tissues are known to be extremely soft and to undergo large deformation under gravity loading. Calvo-Gallego et al. (2015) proposed a uniform polynomial material model for the mixture of adipose and glandular tissues. The authors also shown that the breast outer shape deformation does not depend on glandular distribution but is highly dependent on its volumetric ratio. Here, the glandular and fatty tissues are also modeled as a single homogeneous material with an equivalent Young's modulus  $\lambda_{breast}$ . The mechanical properties of the equivalent breast tissue are in direct relation with glandular and adipose volumes ratios. Because the left and right breasts may have a different granularity, two different parameters are considered ( $\lambda_{breast}^l, \lambda_{breast}^r$ ). have various

Breast skin and superficial fascia are an essential part of the breast support matrix. The two layers are much stiffer than breast tissues and are the structures governing the amount of deformation. Their elastic behavior was included on the optimization process.

Based on existing publications, an interval of possible values are given in table 3.1 for each parameter included in the optimization process ( $\lambda_{breast}^l, \lambda_{breast}^r, \lambda_{skin}, \lambda_{fascia}$ ). To characterize model sensitivity to parameters variations, a set of simulation were performed. The defined interval was discretized by steps of 10% and at each step the skin nodes displacement was computed. Results of the corresponding simulations are shown on Figure 3.14. As previously, the first column represents the variation of mean and maximal displacements

of skin nodes in function of the elastic parameter of each material; the second column represents the change rate and the cumulative change rate of skin nodes displacement

	Search intervals from bibliographic data			Search intervals after model simplification		
	Breast	Skin	Fascia	Breast	Skin	Fascia
Min (kPa)	0.3	7.4	100	0.3	2	50
Max (kPa)	6	58.4	5000	4	20	250

Table 3.1: Minimal and maximal value (in kPa) for Young's modulus.

The figure shows that the model is very sensitive to the variation of Young's modulus of breast tissue, skin and fascia (Figure 3.14). However, beyond some values, the materials become too stiff and do not change significantly under gravity loadings. Therefore, the search intervals for breast tissue and skin Young's modulus are reduced such that a larger value impacts the cumulative change rate less than 20% (max displacement less than  $\sim 5\text{mm}$ ). As the fascia stiffness governs the lateral displacement and shows a smaller variation over the search interval, a threshold of 10 % ( $\sim 2.5\text{mm}$ ) is chosen. The obtained results are summarized in table 3.1

respectively for breast, skin and fascia tissues.

### 3.6.2 Estimation of optimal constitutive parameters

To perform the optimization process, the new intervals defined by sensitive analysis are discretized by steps of  $0.1\text{kPa}$ ,  $1\text{kPa}$  and  $40\text{kPa}$ . The discretization step is chosen such that the change rate between two consecutive simulations is less than 10%.

The previously described multi-loading gravity process was performed for each parameters set and the model error distribution is shown in fig 3.15. The contour lines are estimated by linear interpolation between two consecutive succeeded simulations. We found that the breast tissues Young's modulus is lower than the ones proposed in the bibliography, therefore more simulations were done outside the defined intervals. However, for very low values, below  $0.2\text{kPa}$ ,  $2\text{kPa}$  and  $80\text{kPa}$  for breast, skin and fascia's Young's moduli respectively, the tissues deformation is too large and the finite element mesh becomes degenerated at the first step of the multi-loading simulation. For values above  $1\text{kPa}$ ,  $5\text{kPa}$  and  $160\text{kPa}$ , tissues deformation is too small compared to the ones measured on the MR images and the simulations were excluded. All other missing values correspond to failed simulations due to a non-converging force, specifically in the region of the contact surface between the breast and the muscle.

For very soft fascia ( $\lambda_{fascia} = 80\text{kPa}$ ), the lateral displacement of breast tissues is more important than the one measured on MR images. Conversely, for stiff fascia material ( $\lambda_{fascia} = 160\text{kPa}$ ) the amount of sliding is too small, therefore, to match the breast geometry in supine configuration, very low values for Young modulus are required ( $\lambda_{breast} < 0.2\text{kPa}$ ). For such low values, the breast tissues are highly deformed, thus the finite

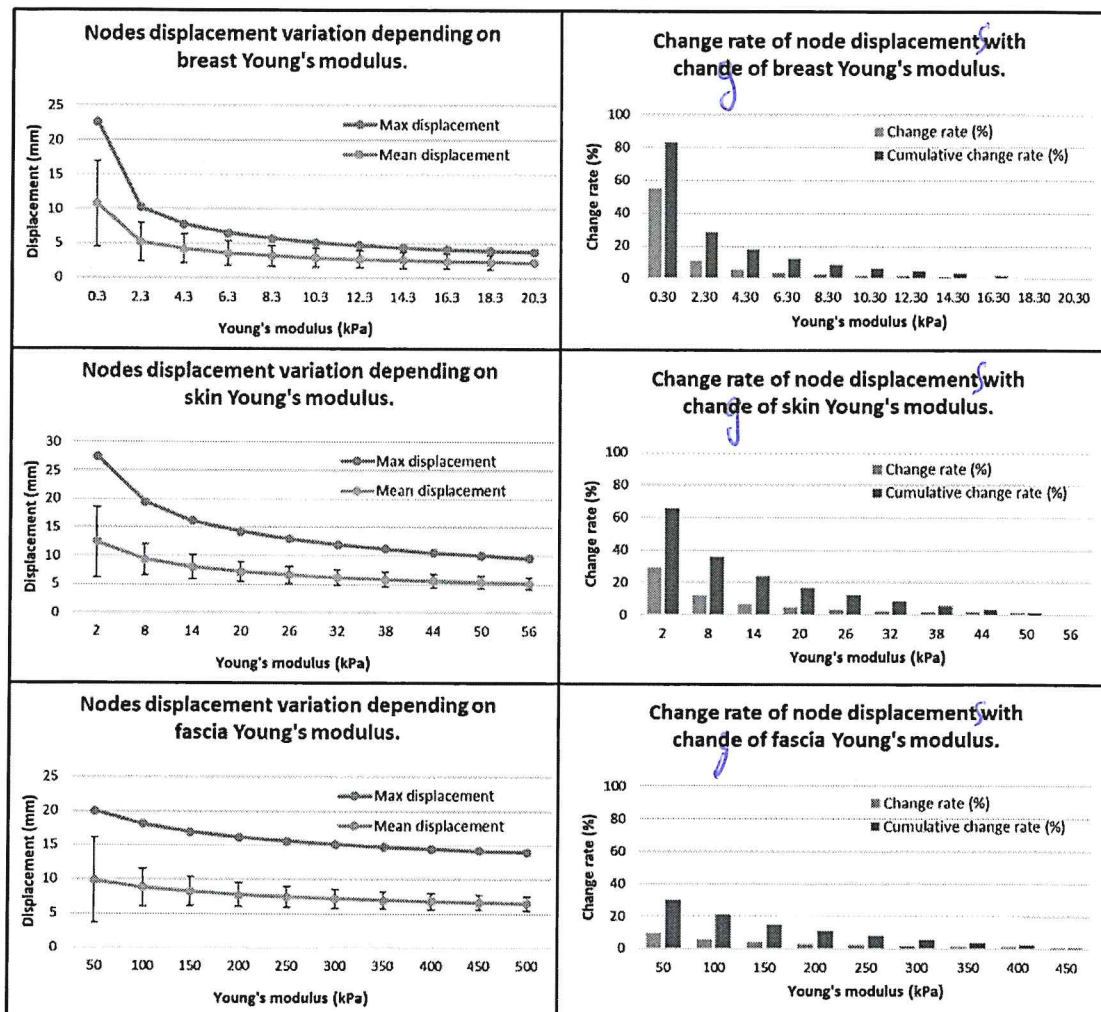


Figure 3.14: First column: relation between maximal and mean nodes displacement and the equivalent Young's modulus variations for different tissues. Second column: rate and cumulative change rate of node displacements in function of equivalent Young's modulus.

elements undergo distortions. Because of errors in elements formulation, the simulations giving the minimal Hausdorff distance have not succeeded.

The set of parameters giving the best match between simulated and measured supine breast configurations is ( $\lambda_{breast}^r = 0.3 \text{ kPa}$ ,  $\lambda_{breast}^l = 0.2 \text{ kPa}$ ,  $\lambda_{skin} = 4 \text{ kPa}$ ,  $\lambda_{fascia} = 120 \text{ kPa}$ ).

mettre *ici une figure superposant les simulations et les mesures en prone et supine.*

### 3.6.3 Conclusion

This chapter propose a new biomechanical breast model. The model was built on patient-specific data extracted from MR images in different breast configurations. New structures as pectoral fascia and suspensory breast ligaments were considered and their impact on

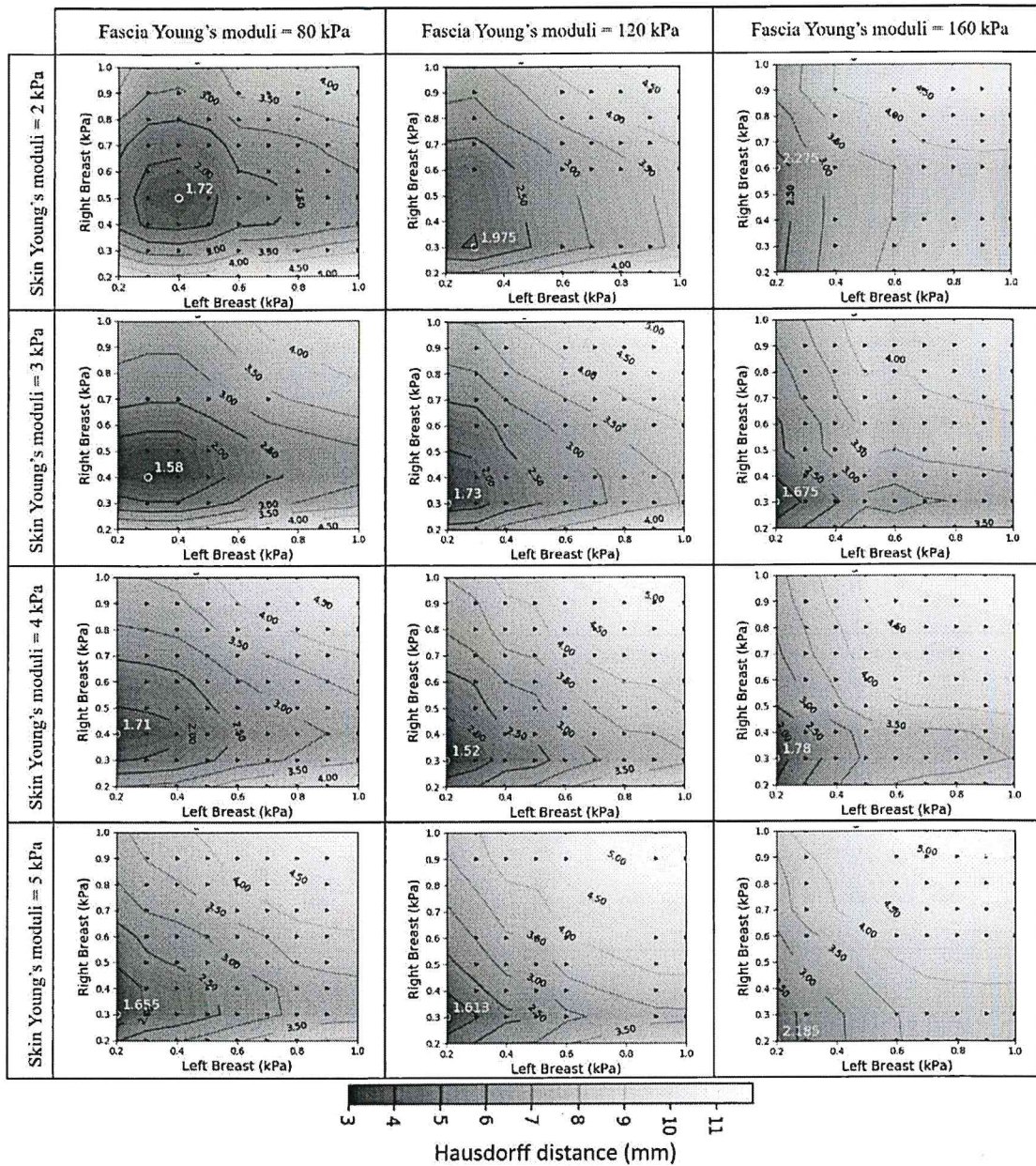


Figure 3.15: Hausdorff distance on the skin surface over the constitutive parameters space.

breast mechanics was analyzed in multi-loading gravity simulations. A particular attention was granted to the estimation of subject-specific breast stress-free geometry and tissues constitutive models.

The proposed breast model shows that introducing a sliding movement of the breast

1710 tissues over the pectoral muscle together with a ligamentous system and pectoral fascia, allows a better estimation of supine and prone configurations. The latter support structures provide a finer method for boundary conditions definition which also improves the

convergence capability of the solution. It can be stated that the obtained Youngs modulus of breast soft tissues <sup>are</sup> relatively low (0.2-0.3kPa for breast tissues and 4kPa for skin), which is a contradictory result compared to some studies on the field. However, only with such small values together with sliding boundary conditions that prone and supine configurations were accurately estimated.

With the obtained optimal constitutive parameters set ( $\lambda_{breast}^r = 0.3kPa, \lambda_{breast}^l = 0.2kPa, \lambda_{skin} = 4kPa, \lambda_{fascia} = 120kPa$ ) and the corresponding breast stress-free configuration simulations with the gravity force oriented in different directions could be simulated. The next chapter evaluate<sup>s</sup> the model accuracy on three breast configurations: supine, prone and supine tilted.

including a

the two prone and supine

Je différencierais les choses. Là tu pourrais cibler les positions prone et supine qui ont été obtenues à partir d'une optimisation  $\rightarrow$  c'est alors normal que les ennuis soient relativement faibles.

Dans le chapitre suivant, là tu évaluerais réellement les performances du modèle pour générer une nouvelle position qui n'a pas été optimisée.

Si tu trouves que le chapitre 4 sera alors trop court, tu pourrais appeler le chapitre 3 "a new biomechanical breast model evaluated on real data". Il faudra alors mettre le chap. 4 dans le chap. 3.

W  
is  
in  
the  
un

# Model validation

## 4.1 Introduction

The previous chapter describes the numerical methods used to develop the breast model and to optimize the patient specific geometrical and mechanical properties. The constitutive parameters giving the best fit between the simulated and measured breast geometries were identified. Knowing the mechanical behavior, the corresponding stress-free geometry is computed and used hereafter as reference configuration for each finite elements simulations. Only the information from MRI volumes in supine and prone configurations were used for the development of the patient-specific model.

MRI-based Previous biomechanical models have used the same MR images for the optimization and evaluation process. In such cases, the model accuracy is assessed for single deformation case, the one used during the optimization process. Because of overfitting problems, the model fidelity to the global breast mechanics independently on the applied gravity direction is poorly described.

The developed breast model is needed to model breast tissues deformation under compression, thus the model error have to be assessed in a more general context. In this chapter the model accuracy is evaluated on supine, prone and supine tilted configuration. The third configuration was not used during the optimization process which allow us to quantify the model accuracy in a more general context than the one used for model optimization.

A reformulation  
(cf. mes remarques  
à la fin de chap.)

## 4.2 Technical approach

The breast reference geometry together with previously defined materials models were used to compute breast deformation under gravity loading. Three loading cases were considered: supine, prone and supine tilted. The body force direction was defined conform to the corresponding vectors obtained by image registration ( section 3.2.3). } idem

To asses the model accuracy to the tissues real deformation, different measures of distance were used:

- Euclidian node to surface distance;
- Mean Euclidian node to surface distance and standard deviation;
- Maximal Euclidian node to surface distance;
- Modified Hausdorff distance;

The detailed description of each distance measure can be found in annex ...

Each distance was computed between simulated and measured skin surfaces. Because the arm position can change between two body positions, the node to surface distance is computed only on the skin nodes belonging to the breast surface. The results for the three body position are presented in the following section.

## 4.3 Results

Figure 4.1 shows node to surface distance magnitude, mean node to surface distance and modified Hausdorff distance between the simulated and measured breast geometries obtained with the optimal sets of parameters for the three previously defined body configurations.

The prone and supine body configurations was used to optimize breast stress-free configuration and material's constitutive parameters. The breast geometry is better estimated in supine configuration with an Hausdorff distance equal to 1.72 mm. This is probably due to a better representation of the boundary conditions in supine configuration, as this configuration was used to create the initial finite element mesh. The breast geometry in prone configuration is also well estimated with a modified Hausdorff distance equal to 2.17 mm. The maximal node to surface distance is obtained on the breast lateral parts. Assuming a non uniform skin thickness or elastic properties over the breast surface as described by Sutradhar and Miller (2013) should improve the obtained results.

One may see that the estimated supine tilted breast configuration describes inadequately the breast geometry given by the MR images (Hausdorff distance equal to 5.90 mm). Large difference between simulated and measured breast surfaces is caused by the excessive sliding of breast tissues over the chest wall. Numerical or structural modeling choices could explain such behavior.

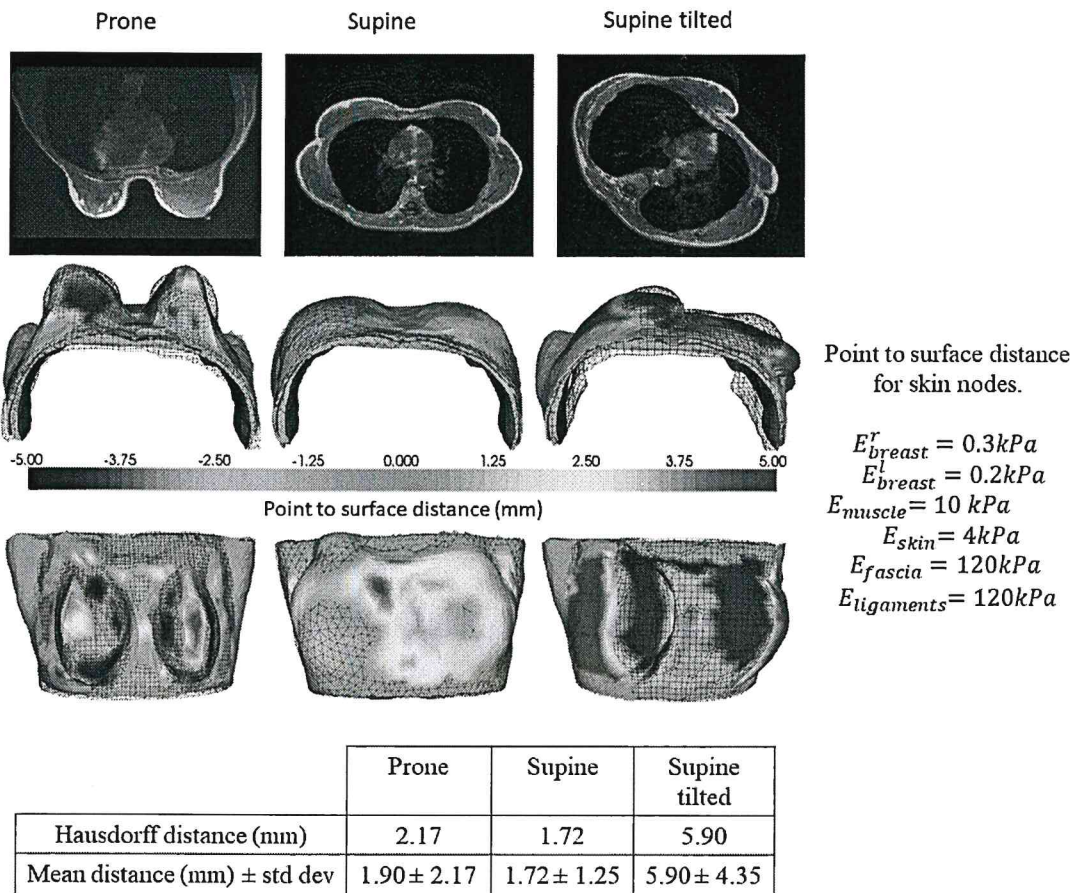


Figure 4.1: Three breast configurations: prone, supine and supine tilted. First line - MR images in 3 breast configurations. Second and third lines - point to node distance from simulated breast shape (surface mesh) to the measured one (black grid lines).

Firstly, the fascial and ligamentous tissues are usually characterized by a cable-like behavior. The strain-energy density function must behave asymptotically in order to limit the fascia stretch and thus to reduce non-linearly the breast sliding over the chest wall. Limitations of the neo-Hookean model to capture the mechanical response of some non-linear materials is well known (Kaliske and Rothert, 1997). For large strain rates, the Neo-Hookean material may undergo a relaxation and therefore becomes easier to deform. Our experimental results have shown that the maximal strain at the fascia level is significantly higher in supine tilted position (about 140%) than in supine or prone positions (about 50%). Therefore, an asymptotic behavior of fascia mechanical response must be considered. The Gent form of strain-energy function characterizes better such mechanical response (Gent, 1996) and should be considered as an alternative choice.

Secondly, the breast support matrix is composed of 4 suspensory ligaments, however only three of them were partially modeled: inframammary, deep medial and deep lateral ligaments. The 3D structures connecting the skin to some muscular areas were neglected,

*Indeed,*

and namely the cranial ligament. The particularity of the cranial ligament consists in its position, almost its entire structure underlays the skin and the only attachments to the thorax are situated at the clavicle and seventh rib levels (inframammary ligament).  
 1795 Including such structures at the skin surface may result in local high strain gradient rates causing solution instability and anesthetic surface deformations.

## 4.4 Discussions and conclusion

In the current part of the manuscript, a new finite elements breast model was proposed and evaluated with real tissues deformations measured on MR images. To this end, MR images 1800 of two patients were acquired in three different configurations: supine, prone and supine tilted. The supine and prone MRI volumes were used to adapt the biomechanical model to the patient individual breast geometry and its respective tissues mechanical properties. The optimal mechanical properties were found by exhaustive search over a predefined 1805 parameters domain. For each combination of tissues elastic properties, the breast reference configuration was computed using an adapted prediction-correction iterative scheme. The parameters set giving the best fit between estimated and measured breast configurations 1810 were selected. Using these optimal estimates, the supine, prone and supine tilted breast configurations were computed and compared to the MRI volumes.  
*works*

*It was* We found that, extremely soft materials low (0.2-0.3kPa for breast tissues and 4kPa for 1815 skin) have to be used in order to obtain the same tissues displacements rate as measured on MR images. Moreover, the breast tissues sliding have to be considered when computing such large deformations. However, because of tissues hyper-elasticity, the model boundary conditions have to be revisited in order to ensure the convergence capability of the solution. With such soft tissues, the finite elements mesh may become highly distorted, then to limit elements distortion, a stiffer layer was added between the breast tissues and muscle representing the deep layer of the superficial fascia. The excessive sliding was prevented by using ligamentous structures fixing the soft tissues on the pectoral muscle.

Contrarily to the previous works, our model is evaluated in 3 breast configurations. Among the 3 geometries, two of them were used for the model optimization and evaluation, and the last one (supine tilted geometry) was used for the evaluation only. Good 1820 estimates were obtained in prone and supine configurations with a Hausdorff distance equal to 2.17mm and 1.72mm respectively. The estimate of the supine tilted breast geometry pointed out the limitations of the Neo-Hookean model to assess rich mechanical behavior of breast soft tissues for large strains. These limitations were not identified in the previous 1825 works.

The model optimization is a tough and time consuming process. It was extremely difficult to obtain the solutions convergence when combining the tissues large deformation with the sliding contact conditions. Because of the lack of time, the reference breast configuration and the optimal constitutive parameters were computed only for the first 1830 subject. The model optimization of the second subject is considered for future work.

Next, we assume that our model describes well the breast mechanical behavior, and is it can

In that case,

be used to compute breast tissues deformation under compression. The internal tissues strain and the pressure distribution over the skin surface will be used to quantify the patient comfort during the mammography exam.

